Effect of Textile-Substrate Pore Size on Electromagnetic Interference Shielding Performance of Conductive Nanocomposite Coated Fabrics

Yijie Hou
Donghua University - Songjiang Campus: Donghua University
Min Guo
Donghua University - Songjiang Campus: Donghua University
Xiangpeng Li
Donghua University - Songjiang Campus: Donghua University
Minghan Duan
Donghua University - Songjiang Campus: Donghua University
Yongtang Jia
Wuyi University
Jianhua Yan
Donghua University - Songjiang Campus: Donghua University
Xianfeng Wang
Donghua University - Songjiang Campus: Donghua University
Ying MA (yingma@dhu.edu.cn)
Donghua University https://orcid.org/0000-0002-6504-2629

Research Article

Keywords: fabric structure, pore size, electromagnetic interference shielding, coating, layer-by-layer assembly, nanocomposite

Posted Date: April 2nd, 2021

DOI: https://doi.org/10.21203/rs.3.rs-344419/v1

Abstract

Textile-substrate electromagnetic interference (EMI) shielding materials show great promise for next-generation electronic communication technology challenges. However, new strategies based on structure optimization are desired for improving EMI shielding performance. Here, we demonstrate the controlling effect of fabric structure on the shielding effectiveness of the EMI fabrics. Plain fabrics with different fabric densities were weaved and used as the substrate to be layer-by-layer assembled by graphite oxide (GO) and polypyrrole (PPy). The conductive GO/PPy nanocomposite coating endows commercial cotton fabrics with an EMI shielding ability. In comparison, the EMI shielding effectiveness of the GO/PPy fabrics is depended on the fabric density, that is, the pore size. The EMI shielding effectiveness of the 100 × 100 picks/ 10cm coated fabric was 19.2 dB in 3.9–6.0 GHz frequency range, which is increased by about 71% through the control of the textile-substrate pore size. Interestingly, the EMI shielding effectiveness always peaks at the fabric density of 100 × 100 picks/ 10cm, different from the electrical conductivity. Moreover, the sueding treatment can further improve the EMI shielding effectiveness of the GO/PPy coated fabrics. It is because that the creation of plush increases the multi-reflection of electromagnetic waves in the fabric. This work presents the significance of fabric structure to EMI shielding performance, offering new opportunities for the development of high efficiency EMI shielding fabrics.

Introduction

Radio-frequency electromagnetic interference (EMI) from computers, mobile phones, the Internet and electronic organizers, often causes undesirable damages to electronic devices and human beings. With the advent of the 5G era, materials capable of shielding against EMI are recognized increasingly due to their applications in reducing and eliminating temporary electronic interference, system failures and data loss (Lian et al. 2020; Liu et al. 2021; Saffer and Thurston 1995; Wang et al. 2020; Yang et al. 2020; Zhao et al. 2020). Textile-substrate EMI shielding materials have been used in civil, commercial, military, and aerospace applications, attributing to the unique characteristics of fabrics such as flexibility, air permeability, wearability (Lee et al. 2016; Li et al. 2018; Wang et al. 2019; Zhu et al. 2021). Coatings of conductive nanocomposites can endow commercial textiles with the capability of shielding against EMI, based on the interactions with electromagnetic waves (Yao et al. 2020; Zhang et al. 2018; Zhao et al. 2017). Under electromagnetic radiation, the nanocomposite coatings generate induced charge carriers (electrons or holes) and transport them by the conductive network, thereby consuming electromagnetic energy. Many efforts have been devoted to the exploration of the coated EMI shielding fabrics, in view of the easy processing and broad application of the coating technologies (Jia et al. 2020; Liu et al. 2019; Zhang et al. 2019). As such, the high-efficiency EMI fabric necessitates excellent electrical conductivity. To this end, increasing the loading content of nanofillers (Cao et al. 2018; Zeng et al. 2016) and optimizing the dispersion and distribution of nanofillers (Verma et al. 2015; Wang et al. 2018) have been employed to enhance the electrical conductivity and EMI shielding performance. Besides of these

approaches, more new strategies are desired to improve EMI shielding for next-generation EMI shielding materials.

Porous structures have been proven to be useful in improving the EMI shielding performance of conductive nanocomposites (Pitkanen et al. 2019; Zeng et al. 2020; Zhang et al. 2020; Zhou et al. 2019). The pores inside a material can induce multi-reflections of electromagnetic waves at their internal interfaces and thus consume additional electromagnetic energy. As the interfacial area increases, the multi-reflection effect grows in magnitude (Chung 2001; Lan et al. 2020; Singh et al. 2018). In order to pursuing the high-efficiency and lightweight EMI shielding materials, a series of researches have been done to investigate the preparation of porous materials and the effect of pore sizes (Jiao et al. 2020; Menon et al. 2018; Zeng et al. 2016). As reported, cellulose-derived carbon aerogels achieved high-efficiency EMI shielding and heat dissipation performance through the small pores and dense three-dimensional sheet-like structure (Zhou et al. 2019). Considering of the porous and complex fabric structures, textile-substrate EMI shielding materials exhibit primary absorption mechanism in electromagnetic loss and are considered as promising next-generation EMI shielding materials (Chen et al. 2020; Gupta et al. 2020; Huang et al. 2019; Zhou et al. 2020). The EMI shielding fabrics have exhibited excellent performance based on the nature of coating materials and the multi-reflection in fabric structures (Ghosh et al. 2019; Ghosh et al. 2018; Ghosh et al. 2020; Ghosh et al. 2018). Woven fabrics possess good structural design ability and dimensional stability and thus have been widely used in household textiles and automobile decorations (Choogin and Valeriy 2013; Michielsen and Lee 2007; zdemir and Baser 2007). Herein, the woven cotton fabrics with different fabric densities were weaved and used as the substrate to be coated with the EMI shielding graphite oxide/ polypyrrole (GO/PPy). We focused on the effect of fabric density on the EMI shielding performance of GO/PPy coated fabrics. The conductive GO/PPy coating has been demonstrated to be useful in providing a satisfactory EMI shielding performance to commercial cotton fabrics, as described in our previous work (Zou et al. 2016). This work showed that the EMI shielding effectiveness of the GO/PPy fabrics is depended on the fabric structure, for example, the fabric density. Interestingly, the EMI shielding effectiveness always peaks when the fabric density is 100 × 100 picks /10cm.

Experimental

Materials

Graphite oxide (GO) powder was provided from XFNANO Materials Tech Co., Ltd (Nanjing). Pyrrole (Py) monomer, ferric chloride ($FeCl_3$•$6H_2O$), sodium hydroxide (NaOH), sodium dodecylbenzene sulfonate (SDBS), and ethanol were purchased from Sinopharm Chemical Reagent Co., Ltd. (3-Chloro-2-hydroxypropyl) trimethylammonium Chloride (CHP_3MAC ca. 65% in Water) was purchased from TCI (Shanghai) Co., Ltd. All chemicals were used without further purification.

Preparation of woven fabrics

The used cotton yarn is made by twisting two single yarns with a fineness of 32 gauzes and was purchased from Miaomiao Yarns (Changzhou). By using an automatic rapier loom (Sakura TNY501C-20), plain cotton fabrics were weaved with different fabric densities, which are 50 × 50, 70 × 70, 100 × 100, 150 × 150, 200 × 200, and 250 × 250 picks/10cm.

Layer-by-layer assembly of GO/PPy coatings

The as-prepared woven cotton fabrics as textile substrates were treated with a mixed solution of 50 g•L^{-1} NaOH and 5 g•L^{-1} SDBS at 60 °C for 2 h for cleaning. Subsequently, the fabrics were immersed into a cationic solution of 50 mg/mL CHP_3MAC and 18 mg/mL NaOH for 24 h to covalently bond cationic EP_3MAC molecules on fiber surfaces, and then washed in deionized water and dried in an oven at 60 °C. The pre-treated fabric with cationic charges was decorated with GO/PPy coatings by dipping into the 0.4 mg/mL GO dispersion for 10 min, 0.5 mol•L^{-1} Py ethanol solution for 10 min, 0.5 mol•L^{-1} $FeCl_3$ solution for 30 min under an ice bath condition. Here, the GO suspension solution was obtained by ultrasonic treatment of GO powder in DI water. Washing steps were conducted after each dipping step to remove additional physical adsorption. And all fabrics were dried in an oven.

Characterization

Photographs of uncoated and coated woven fabrics were captured by a camera (Canon PC1680). The morphologies were obtained by an optical microscope (Nikon Eclipse LV100POL) and SEM (Hitachi S-4800). EMI shielding performance of fabrics was measured by a vector network analyzer (Rohde & Schwarz ZVL6) in 3.9-6 GHz frequency ranges. The surface resistances of fabrics were measured a digital multimeter (FLUKE 15B) according to AATCC test method 76–2005. The capillary flow analysis was conducted by a PMI capillary flow porometer (Porous Materials Inc. CFP-1100AI).

Results And Discussion

Plain fabrics with a same warp density and weft density were chosen as the fabric substrate to investigate the effect of fabric structures on the EMI shielding performance of the coated fabrics. As shown in Figure 1a, the pore size can be controlled by the fabric density. In this work, the plain weave fabric adopts 32s /2 cotton yarns, which refers to the double-ply yarn with a fineness of 32 gauzes in English count. The average value of yarn diameter was determined to be 285.6 μm, as shown in Figure 1b. The double yarns were weaved to the plain fabrics with different fabric densities, which are 50 × 50, 70 × 70, 100 × 100, 150 × 150, 200 × 200, and 250 × 250 picks/10cm. The obtained plain fabrics were denoted as S50, S70, S150, S200, and S250. The structure of the fabric and the change of the pore size can be clearly observed by microscope, as shown in Figure 1c. With the increase of the fabric density, the pores created by interlacing the warp and weft yarns became smaller. The pore size of S50 cannot be shown completely in the microscopy image, because a single fabric structure unit is larger than the field of the microscope. From S70 to S150, the average pore sizes were determined to be 960.6, 660.3, 158.9, 63.7 and 22.3 μm. Besides, theoretical pore sizes were calculated based on the fabric density and the

yarn diameter, assuming the pores are uniform and straight round. The theoretical results were 1714.4, 1144.4, 714.4, 384.4, 214.4 and 114.4 μm, respectively. The theoretical and experimental results both were drawn in Figure 1d, exhibiting a similar trend as a function of fabric density, where the warp density is always same with the weft density. All experimental data are smaller than the theoretical, attributing to the flexibility and mobility of yarns.

The plain-woven cotton fabric as the substrate was layer-by-layer assembled by GO/PPy for EMI shielding, as illustrated in Figure 2a. The pretreated fabric with positive charges was alternately immersed in a 0.2 mg mL^{-1} GO dispersion, 0.5 mol L^{-1} pyrrole ethanol solution and 0.5 mol L^{-1} ferric chloride aqueous solution. The deposition steps could be repeated until a desired film is obtained. The coating after 5 deposition cycles was denoted as (GO/PPy)*5. The used GO sheets were obtained by exfoliating GO powder. Figure 2b shows two Raman characteristic peaks of GO sheets, corresponding to the D band at 1350 cm^{-1} and the G band at 1601 cm^{-1}. The XRD pattern of the GO sheets in Figure 2c exhibites a sharp peak at 2θ=10.8°, indicating that the *d*-spacing was 8.2 Å. The result is consistent with that of AFM (Figure 2d), in which the thickness of a GO sheet was determined to be 8.9 nm. The thickness is larger than that of graphite sheets of 3.35 Å, because of the oxygen-containing groups on surfaces. The in-situ polymerized PPy can be absorbed on the GO layer through the electrostatic and $\pi-\pi^*$ interactions between PPy and GO. Elemental analysis of the resulting GO/PPy coating on a cotton fabric was conducted by X-ray photoelectron spectroscopy (XPS). As shown in Figure 2e, the survey-scanning XPS spectra displayed three characteristic peaks of carbon (C 1s, 286.0 eV), oxygen (O 1s, 532.4 eV) and nitrogen (N 1s, 393.6 eV), which belong to the GO and PPy. The N 1s can be deconvoluted to two peaks at 393.1 and 401.7 eV. The peak at 401.7 eV corresponds to the binding energy for quaternary ammonium groups, which can interact with GO by electrostatic interaction (Ma et al. 2007) The obtained (GO/PPy)*5 fabric (Figure 2f) remained the softness and air permeability of the uncoated cotton fabric, but changed in color to black. From the scanning electron microscopy (SEM) images in Figure 2g and h, the (GO/PPy)*5 coating covered the surface of each fiber and increased the surface roughness but maintained the original morphological feature of cotton fibers. Besides, a layered structure within the GO/PPy coating was constructed by GO sheets, as described in our previous work (Zou et al. 2016).The conductive polymer of PPy provides the necessary conductive network to EMI shielding, while the GO sheets acts as separators to multireflect electromagnetic waves in the coating. The layered GO/PPy coating has been proven to be highly efficient to prolong the propagation path of electromagnetic waves and accelerate the heat dissipation. Combined with the porous fabric structure, electromagnetic waves can multi-interact with the high efficiency GO/PPy coating, resulting in an excellent EMI absorption performance.

In order to investigate the effect of fabric structures on the EMI shielding, the plain-woven fabrics with different fabric densities were assembled by the (GO/PPy)*n (n=1 to 5) and compared in electrical conductivity and EMI shielding performance. Considering that the main shielding mechanism of EMI materials is dielectric loss, electrical conductivity of materials is an important index to estimate EMI performance. The surface resistance of these coated fabrics was measured to present their electrical

conductivity, as illustrated in Figure 3a. The surface resistance of the coated fabrics decreases, i.e. the conductivity increases, with the assembly of GO/PPy. Meanwhile, the surface resistance decreases with the increase of fabric density, at the same deposition cycles of GO/PPy. It is because that the number of conductive paths increases. It is worth noting that the effect of fabric density on the conductivity get weaken with the thickening of the conductive GO/ PPy coating. EMI shielding effectiveness (SE), which is a critical factor to evaluate the shielding performance of materials, is the logarithmic ratio of the transmitted electromagnetic power (P_t) through the material to the incident electromagnetic power (P_i), i.e. (Gahlout and Choudhary 2019). The EMI SE of the coated fabrics in 3.9–6.0 GHz frequency range (C band) was measured. The C band is an important frequency band widely used in Wi-Fi devices and wireless phones. The average EMI SE in 3.9–6.0 GHz was calculated and shown in Figure 3b. Like the electrical conductivity, the SE value also increases with the assembly of GO/PPy. The difference is that the SE value of coated fabrics is maximum at 100 × 100 picks/10cm. For different deposition cycles of GO/PPy, the trend is same. The SE of the (GO/PPy)*5 fabric at 100 × 100 picks/10cm was close to 20 dB, which is the standard of EMI shielding materials to meet the requirement for commercial applications. More importantly, the maximum shielding performance of the coated fabrics with different layer numbers always appears at the same fabric density of 100 × 100 picks/10cm, indicating that the pore size of fabrics plays an important role in the EMI shielding performance of textile-substrate materials. The EMI SE at 100 × 100 picks/10cm (19.2 dB) was increased by about 71%, compared to that of 250 × 250 picks/10cm (11.2 dB). We further analyzed the reflection loss (SE_r) and absorption loss (SE_a) of the GO/PPy coated fabrics, as show in Figure 3c. By contrast, SE_a accounts for a large proportion of the total EMI attenuation. It indicated that the main shielding mechanism is absorption, which is admirable for reducing the secondary damage of electromagnetic waves. The ratios of SE_a to the total EMI attenuation maintained at a high level, that is, the shielding mechanism of the GO/PPy coated fabric is always absorption. Additionally, the ratio of SE_a was similar for different fabric densities, for example, that is always ~84% for the (GO/PPy)*5 coated fabric. The results indicated that the peak at 100 × 100 picks/10cm is attributed to that appropriate fabric pores prolong the propagation path of electromagnetic waves in fabrics.

In order to investigate the effect of fabric structures on the EMI shielding performance, the pore sizes of the uncoated and coated fabrics with (GO/PPy)*3 were analyzed by capillary flow porometer. Fabrics are known to have complex and hierarchical structures. The fabric pores has a hierarchical distribution, including 0.2~200 μm pores between fibers and 20~1000 μm pores between yarns. Commonly, the fabric pore are permeable. From Figure 4, the plain-woven cotton fabric at 100 × 100 picks/ 10cm has been proven to possess hierarchical porosity. They were distributed in the range of 40~140 μm and 180~380 μm. After 3 deposition cycles of GO/PPy, the pore size decreased obviously and were distributed in the rage of 4.7~300 μm. It was attributed to the deposition of GO/PPy and the deformation of fabric structure after the wet assembly and drying step. The wide range of fabric pore sizes makes it difficult to determine which pore matches the wavelength of electromagnetic waves, resulting in an increase in electromagnetic shielding. As depicted in Figure 5, the GO/PPy build a representative layered conductive coating on the fabric, where the conductive polymer of PPy forms a conducting network to efficient carry

charge carriers and attenuate electromagnetic energy, whereas the GO sheets with a poor conductivity act as nanoseparators to change the direction of electromagnetic waves and prolong the paths of electromagnetic waves. When electromagnetic waves hits a GO/PPy coated fiber, a part of electromagnetic waves is absorbed and a part is reflected off. The high efficiency GO/PPy coating generates an excellent EMI shielding performance through the multi-reflection of porous fabric against electromagnetic waves. The incident electromagnetic waves were reflected multiple times and acted with the GO/PPy coating multiple times, leading to the shielding mechanism of absorption.

We further conducted the sueding on the plain-woven cotton fabrics to investigate its influence on the EMI shielding performance. According to GB/T 4802.1-2008 fabric pilling performance test, the fabrics were forced to grind with the abrasive under a certain pressure, so that the fibers in the yarn were pulled out, shifted and broken, and plush was produced. The plain-woven cotton fabrics at 100 × 100 picks/10cm before and after sueding as examples were shown in Figure 6a and b. The microscopic images show that the surface of the fabric is relatively flat with a small amount of hairiness. After sueding, a large number of long fibers appeared on the fabric surface, and the long fibers were basically perpendicular to the fabric surface. Meanwhile, the thickness of the suede treated fabric looks to be reduced, because the yarn structure of the fabric is loosened by the sueding treatment. Subsequently, the plain-woven cotton fabrics with different fabric densities were layer-by-layer assembled by a (GO/PPy)*3 coating. The EMI shielding performance was measured and shown in Figure 6a. The peaks of EMI SE were found in both single-sided and double-sided sueding samples when the fabric density was 100 × 100 picks / 10cm. In addition, the SE values of the fabrics after sueding are all higher. It is attributed to the creation of plush, which increases the multi-reflection of electromagnetic waves in the fabric. In comparison, the SE value of the double-sided sueding samples were slightly higher than the single-side samples but fluctuated markedly. It is also because that the sueding treatment makes the yarn structure of the fabric loose and even break.

Conclusions

In summary, we have demonstrated the effect of fabric structure on the shielding effectiveness of the EMI fabrics. The plain fabrics with different fabric densities were weaved and used as the substrate to be layer-by-layer assembled by graphite oxide (GO) and polypyrrole (PPy). The conductive GO/PPy coating endowed commercial fabrics with an EMI shielding ability. In comparison, the EMI shielding effectiveness of the GO/PPy fabrics was depended on the fabric density. Interestingly, the EMI shielding effectiveness always possessed a maximum at the fabric density of 100 × 100 picks/ 10cm, different from the electrical conductivity. Moreover, the sueding treatment was conducted to further improve the EMI shielding effectiveness of the GO/PPy fabrics. It is because that the creation of plush can increase the multi-reflection of electromagnetic waves in the fabric. This work presents the important effect of fabric structure on the EMI shielding performance, offering new opportunities for the development of high efficiency EMI shielding fabrics.

Declarations

Funding This work was supported by the Fundamental Research Funds for the Central Universities (No. 2232021G-01), National Key Research and Development Program of China (No. 2018YFC2000900), the Key Program of Educational Commission of Guangdong Province (Nos. 2019KZDXM017 and 2018KZDXM071), the Outstanding Youth Foundation of Guangdong Province of China (No.2018 B030306020), and the Key Applied Research Projects of Guangdong Province (No.2018KZDXM 071).

Conflicts of interest The authors declare no competing financial interest.

Availability of data and material Not applicable

Code availability Not applicable

Authors' contributions

Yijie Hou: Data curation, Writing - original draft.

Min Guo: Investigation.

Xiangpeng Li: Investigation.

Minghan Duan: Investigation.

Yongtang Jia: Supervision.

Jianhua Yan: Resources.

Xianfeng Wang: Resources.

Ying Ma: Conceptualization, Writing - review & editing.

Ethics approval Not applicable

References

Cao WT, Chen FF, Zhu YJ, Zhang YG, Jiang YY, Ma MG, Chen F (2018) Binary Strengthening and Toughening of MXene/Cellulose Nanofiber Composite Paper with Nacre-Inspired Structure and Superior Electromagnetic Interference Shielding Properties ACS Nano 12:4583-4593

Chen L, Guo K, Zeng SL, Xu L, Xing CY, Zhang S, Li BJ (2020) Cross-stacking aligned non-woven fabrics with automatic self-healing properties for electromagnetic interference shielding Carbon 162:445-454

Choogin, Valeriy V (2013) Woven fabric formation: principles and methods.

Chung DDL (2001) Electromagnetic interference shielding effectiveness of carbon materials Carbon 39:279-285

Gahlout P, Choudhary V (2019) Microwave shielding behaviour of polypyrrole impregnated fabrics Composites Part B-Engineering 175

Ghosh S, Das P, Ganguly S et al. (2019) 3D-Enhanced, High-Performing, Super-hydrophobic and Electromagnetic-Interference Shielding Fabrics Based on Silver Paint and Their Use in Antibacterial Applications. ChemistrySelect 4:11748-11754

Ghosh S, Mondal S, Ganguly S et al. (2018) Carbon Nanostructures Based Mechanically Robust Conducting Cotton Fabric for Improved Electromagnetic Interference Shielding. Fibers and Polymers 19:1064-1073

Ghosh S, Nitin B, Remanan S et al. (2020) A Multifunctional Smart Textile Derived from Merino Wool/Nylon Polymer Nanocomposites as Next Generation Microwave Absorber and Soft Touch Sensor. ACS Appl Mater Interfaces 12:17988-18001

Ghosh S, Remanan S, Mondal S et al. (2018) An approach to prepare mechanically robust full IPN strengthened conductive cotton fabric for high strain tolerant electromagnetic interference shielding. Chemical Engineering Journal 344:138-154

Gupta S, Chang C, Anbalagan AK, Lee CH, Tai NH (2020) Reduced graphene oxide/zinc oxide coated wearable electrically conductive cotton textile for high microwave absorption Composites Science And Technology 188:9

Huang L, Li JJ, Li YB, He XD, Yuan Y (2019) Fibrous Composites with Double-Continuous Conductive Network for Strong Low-Frequency Microwave Absorption Ind Eng Chem Res 58:11927-11938

Jia LC et al. (2020) Stretchable Liquid Metal-Based Conductive Textile for Electromagnetic Interference Shielding Acs Applied Materials & Interfaces 12:53230-53238

Jiao YZ et al. (2020) Conjugate Microporous Polymer-Derived Conductive Porous Carbon Nanoparticles with Narrow Pore-Size Distribution for Electromagnetic Interference Shielding Acs Applied Nano Materials 3:4553-4561

Lan CT, Zou LH, Qiu YP, Ma Y (2020) Tuning solid-air interface of porous graphene paper for enhanced electromagnetic interference shielding Journal Of Materials Science 55:6598-6609

Lee SE, Lee WJ, Oh KS, Kim CG (2016) Broadband all fiber-reinforced composite radar absorbing structure integrated by inductive frequency selective carbon fiber fabric and carbon-nanotube-loaded glass fabrics Carbon 107:564-572

Li X, Li Y, Guan TT, Xu FC, Sun JQ (2018) Durable, Highly Electrically Conductive Cotton Fabrics with Healable Superamphiphobicity Acs Applied Materials & Interfaces 10:12042-12050

Lian YL et al. (2020) Solvent-Free Synthesis of Ultrafine Tungsten Carbide Nanoparticles-Decorated Carbon Nanosheets for Microwave Absorption Nano-Micro Letters 12

Liu HG, Wu SQ, You CY, Tian N, Li Y, Chopra N (2021) Recent progress in morphological engineering of carbon materials for electromagnetic interference shielding Carbon 172:569-596

Liu LX, Chen W, Zhang HB, Wang QW, Guan FL, Yu ZZ (2019) Flexible and Multifunctional Silk Textiles with Biomimetic Leaf-Like MXene/Silver Nanowire Nanostructures for Electromagnetic Interference Shielding, Humidity Monitoring, and Self-Derived Hydrophobicity Advanced Functional Materials 29:10

Ma Y, Sun J, Shen J (2007) Ion-triggered exfoliation of layer-by-layer assembled poly(acrylic acid)/poly(allylamine hydrochloride) films from substrates: A facile way to prepare free-standing multilayer films Chemistry Of Materials 19:5058-5062

Menon AV, Madras G, Bose S (2018) Shape memory polyurethane nanocomposites with porous architectures for enhanced microwave shielding Chemical Engineering Journal 352:590-600

Michielsen S, Lee HJ (2007) Design of a superhydrophobic surface using woven structures Langmuir the Acs Journal of Surfaces & Colloids 23:6004-6010

Pitkanen O, Tolvanen J, Szenti I, Kukovecz A, Hannu J, Jantunen H, Kordas K (2019) Lightweight Hierarchical Carbon Nanocomposites with Highly Efficient and Tunable Electromagnetic Interference Shielding Properties Acs Applied Materials & Interfaces 11:19331-19338

Saffer JD, Thurston SJ (1995) CANCER RISK AND ELECTROMAGNETIC-FIELDS Nature 375:22-23

Singh AK, Shishkin A, Koppel T, Gupta N (2018) A review of porous lightweight composite materials for electromagnetic interference shielding Composites Part B-Engineering 149:188-197

Verma P, Saini P, Malik RS, Choudhary V (2015) Excellent electromagnetic interference shielding and mechanical properties of high loading carbon-nanotubes/polymer composites designed using melt recirculation equipped twin-screw extruder Carbon 89:308-317

Wang GH, Ong SJH, Zhao Y, Xu ZJC, Ji GB (2020) Integrated multifunctional macrostructures for electromagnetic wave absorption and shielding Journal Of Materials Chemistry A 8:24368-24387

Wang GL et al. (2018) Ultralow-Threshold and Lightweight Biodegradable Porous PLA/MWCNT with Segregated Conductive Networks for High-Performance Thermal Insulation and Electromagnetic Interference Shielding Applications Acs Applied Materials & Interfaces 10:1195-1203

Wang QW et al. (2019) Multifunctional and Water-Resistant MXene-Decorated Polyester Textiles with Outstanding Electromagnetic Interference Shielding and Joule Heating Performances Advanced Functional Materials 29

Yang Y et al. (2020) Reduced Graphene Oxide Conformally Wrapped Silver Nanowire Networks for Flexible Transparent Heating and Electromagnetic Interference Shielding ACS Nano 14:8754-8765

Yao B et al. (2020) Highly Stretchable Polymer Composite with Strain-Enhanced Electromagnetic Interference Shielding Effectiveness Advanced Materials 32

zdemir H, Baser G (2007) Computer Simulation of Woven Structures Based on Actual Yarn Photographs. Springer Berlin Heidelberg.

Zeng ZH, Jin H, Chen MJ, Li WW, Zhou LC, Zhang Z (2016) Lightweight and Anisotropic Porous MWCNT/WPU Composites for Ultrahigh Performance Electromagnetic Interference Shielding Advanced Functional Materials 26:303-310

Zeng ZH et al. (2020) Nanocellulose assisted preparation of ambient dried, large-scale and mechanically robust carbon nanotube foams for electromagnetic interference shielding Journal Of Materials Chemistry A 8:17969-17979

Zhang JP et al. (2020) Homogeneous silver nanoparticles decorating 3D carbon nanotube sponges as flexible high-performance electromagnetic shielding composite materials Carbon 165:404-411

Zhang Q et al. (2018) Electromagnetic Shielding Hybrid Nanogenerator for Health Monitoring and Protection Advanced Functional Materials 28

Zhang Y et al. (2019) Eco-friendly flame retardant and electromagnetic interference shielding cotton fabrics with multi-layered coatings Chemical Engineering Journal 372:1077-1090

Zhao H, Hou L, Bi SY, Lu YX (2017) Enhanced X-Band Electromagnetic-Interference Shielding Performance of Layer-Structured Fabric-Supported Polyaniline/Cobalt-Nickel Coatings Acs Applied Materials & Interfaces 9:33059-33070

Zhao HH et al. (2020) Heterogeneous Interface Induced the Formation of Hierarchically Hollow Carbon Microcubes against Electromagnetic Pollution Small 16

Zhou XF et al. (2020) Synthesis of porous carbon embedded with NiCo/CoNiO2 hybrids composites for excellent electromagnetic wave absorption performance J Colloid Interface Sci 575:130-139

Zhou ZH et al. (2019) Structuring dense three-dimensional sheet-like skeleton networks in biomass-derived carbon aerogels for efficient electromagnetic interference shielding Carbon 152:316-324

Zhu S et al. (2021) Multi-functional and highly conductive textiles with ultra-high durability through 'green' fabrication process Chemical Engineering Journal 406:10

Zou LH, Zhang SL, Li XP, Lan CT, Qiu YP, Ma Y (2016) Step-by-Step Strategy for Constructing Multilayer Structured Coatings toward High-Efficiency Electromagnetic Interference Shielding Advanced Materials Interfaces 3

Figures

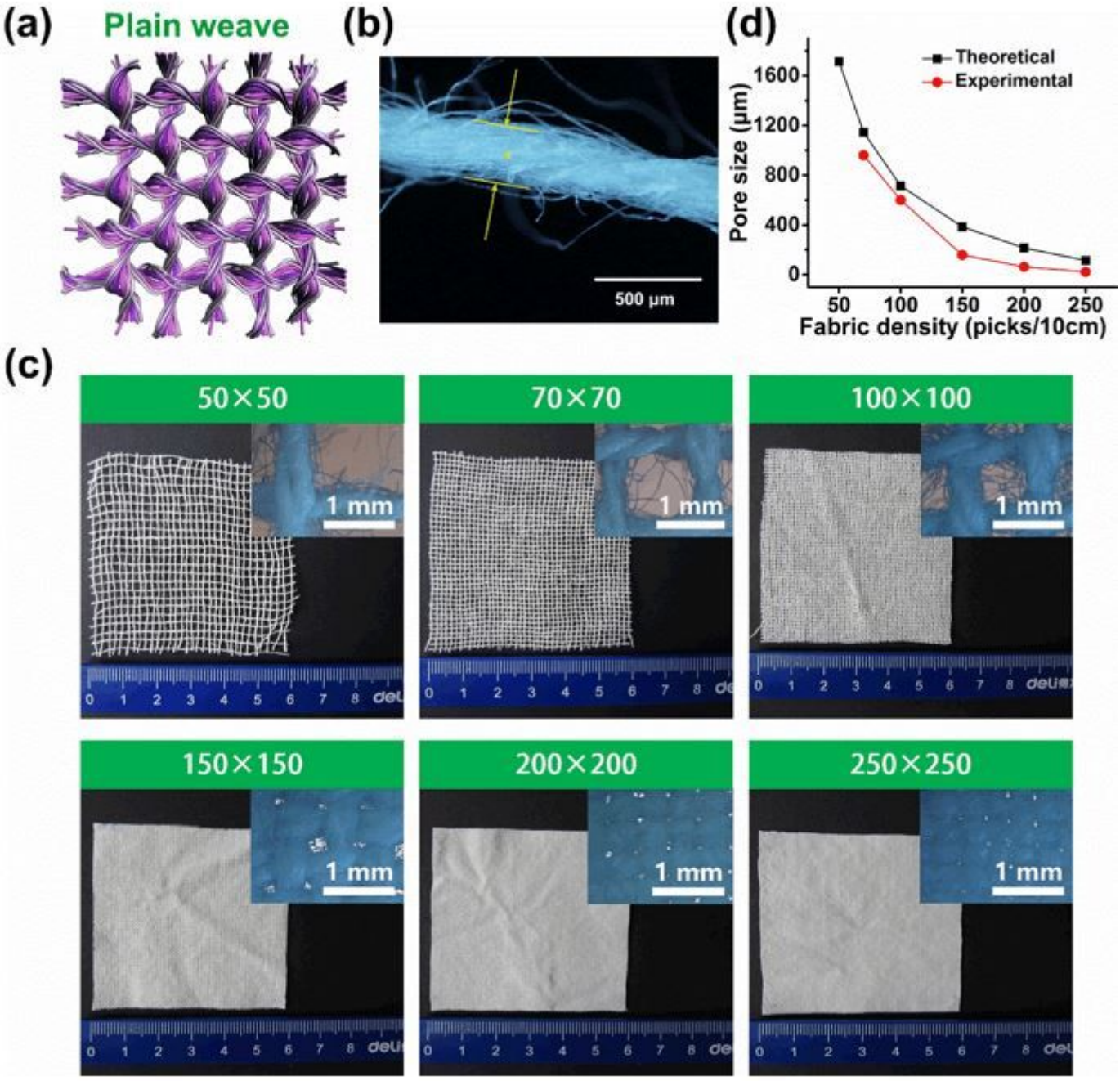

Figure 1

(a) Structural schematics of the plain woven fabric. (b) Microscopy image of a 32s/2 cotton yarn. (c) Optical pictures and microphotographs (insets) of the obtained woven fabrics with different fabric densities. (d) Evolution of pore size of the woven fabrics with the increase of fabric density.

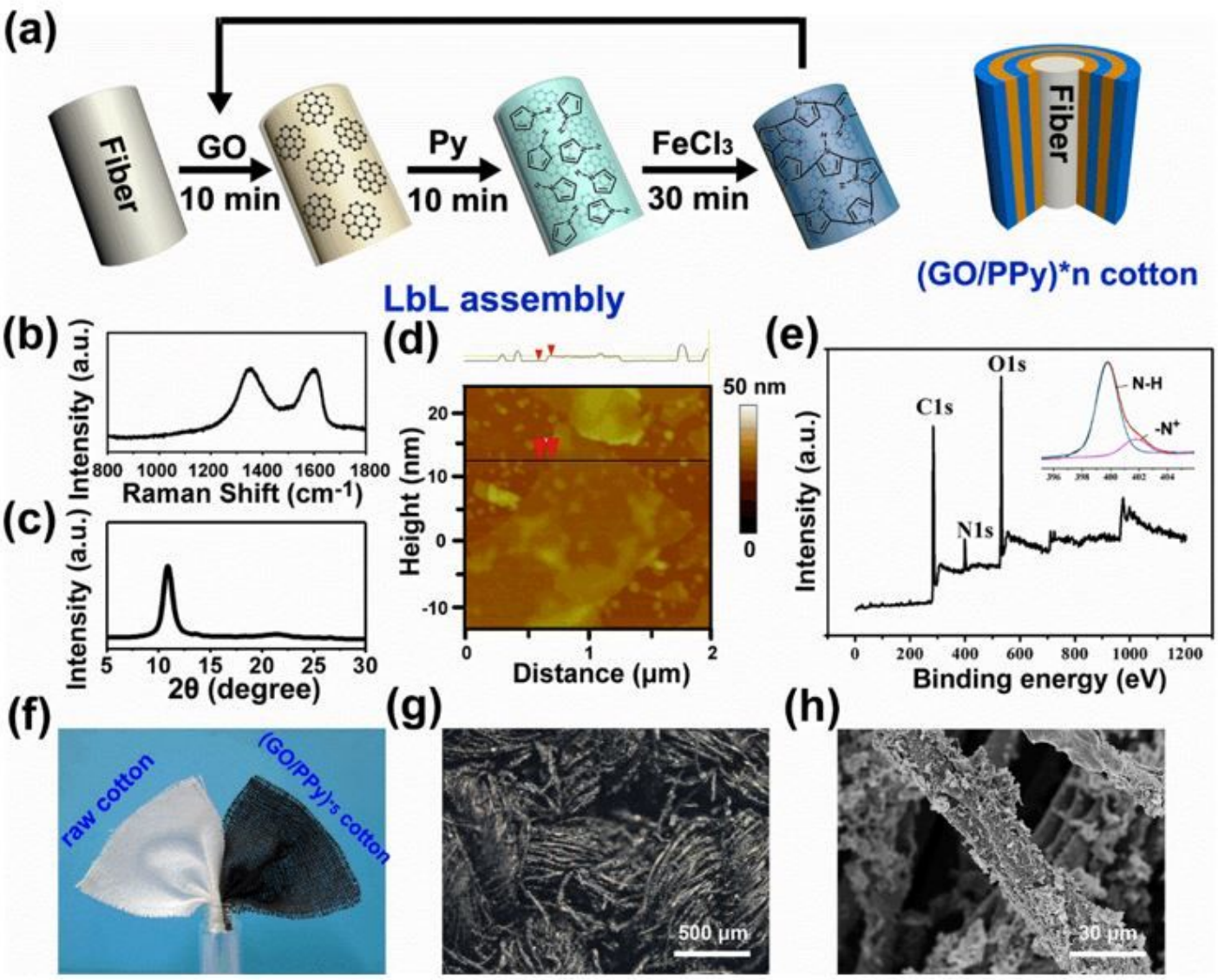

Figure 2

(a) Schematic illustration of the layer-by-layer assembly procedure of the GO/PPy on fabrics. (b) Raman spectrum and (c) XRD pattern of the used GO sheets. (d) AFM image and height profile of a GO sheet. (d) XPS N 1s spectrum of in-situ polymerized PPy in an ice bath. (e) XPS spectra of the GO/PPy coating. (f) Photographs of the uncoated and coated fabrics (70 × 70 picks/10cm) with the (GO/PPy)*5. (g) Microphotograph and (h) SEM image of the (GO/PPy)*5 fabric (70 × 70 picks/10cm).

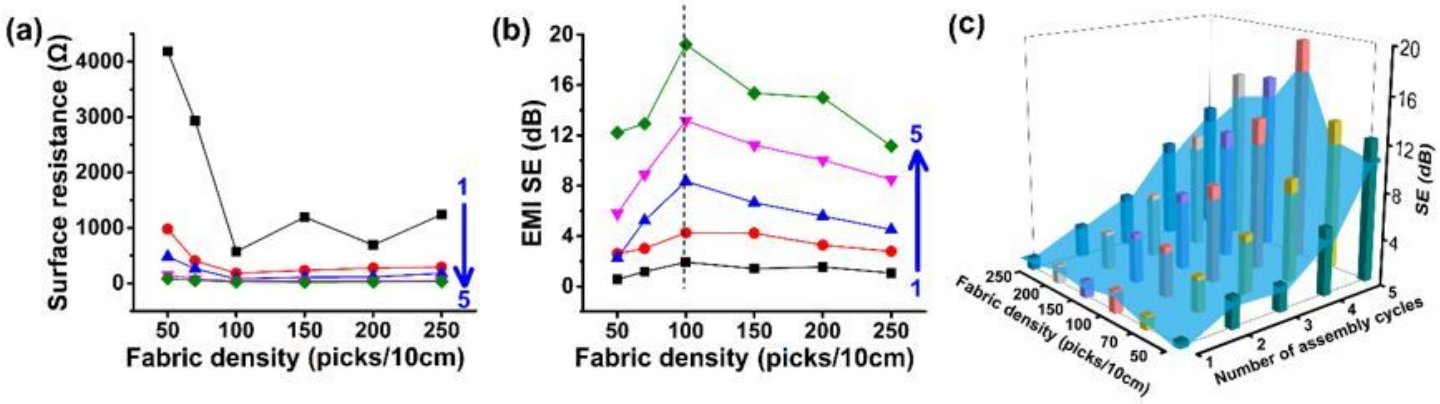

Figure 3

(a) Surface resistance values, (b) EMI SE values and (c) Shielding indexes of the woven fabrics covered with a (GO/PPy)*n coating (n=1~5).

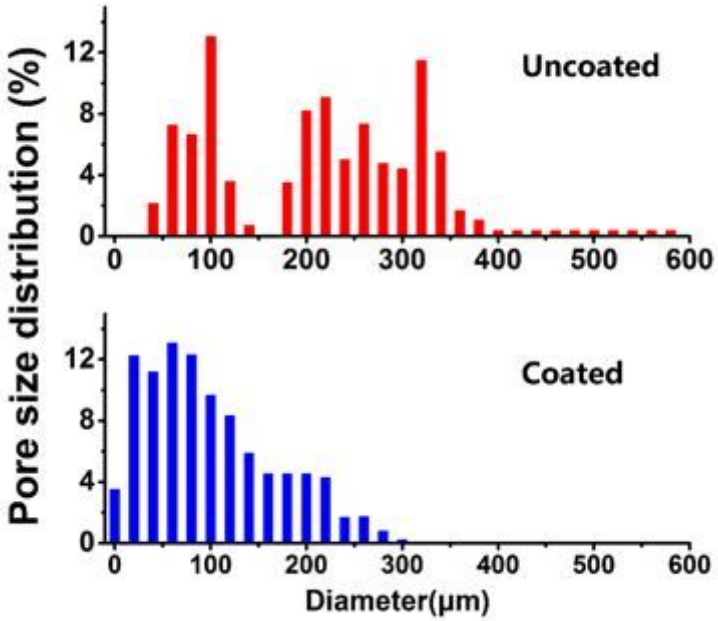

Figure 4

Pore size distributions of the uncoated and coated fabrics (100 × 100 picks/10cm) with a (GO/PPy)*3 coating.

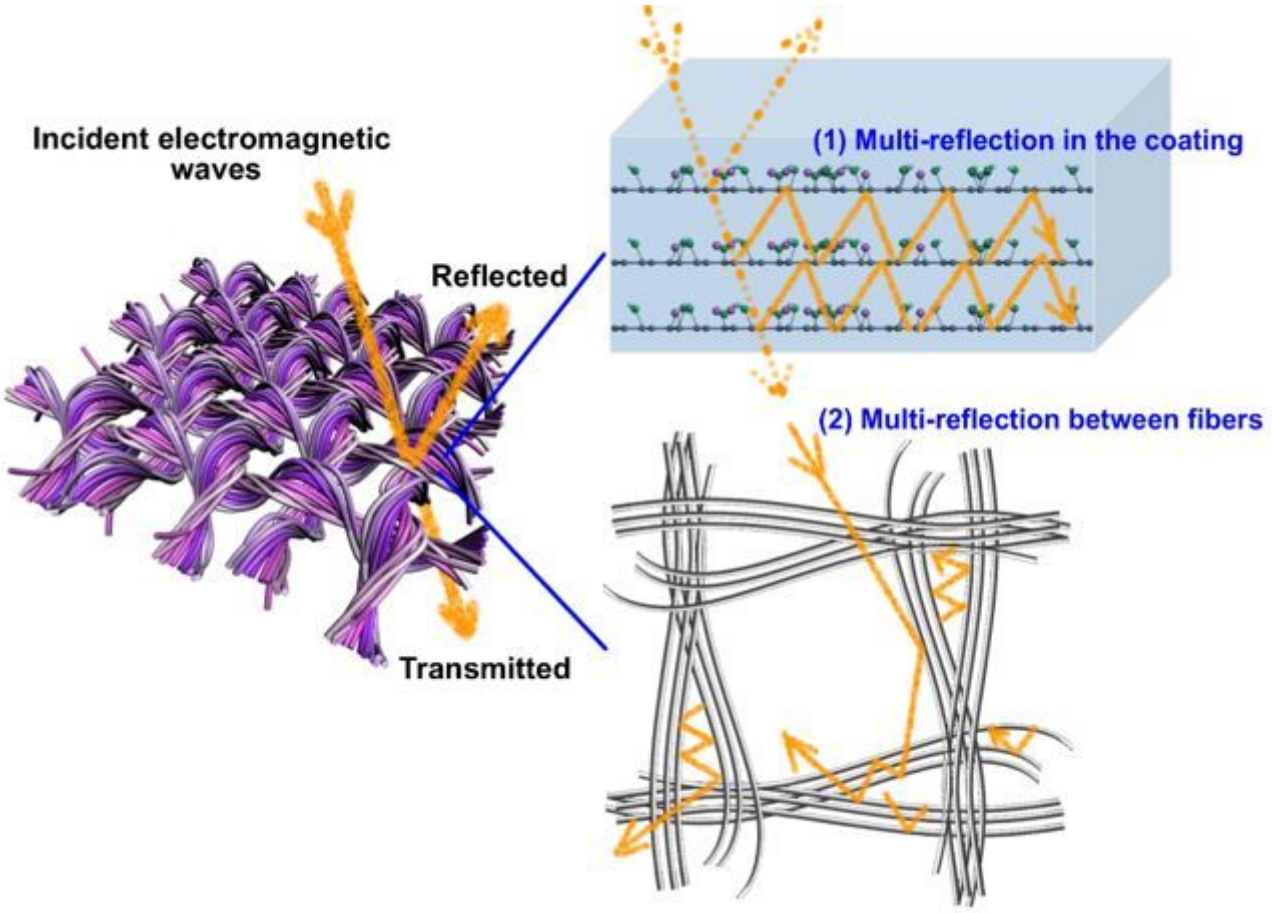

Figure 5

Schematically depiction of EMI shielding on the CNT coated fabric.

Figure 6

Optical images of the woven fabric (a) before sueding and (b) after sueding. (c) EMI SE values of the (GO/PPy)*3 fabrics under different sueding conditions.